On the possibility of demonstrating ionization cooling with proton beams on an internal hydrogen target in the IOTA ring at the Fermilab ASTA facility

V. Shiltsev, V. I. Balbekov, M. Chung, G. Stancari,* and A. Valishev

Fermi National Accelerator Laboratory, P.O. Box 500, Batavia, Illinois 60510, USA†

(Dated: February 17, 2013)

We consider a demonstration of the ionization cooling principle using 2.5-MeV protons interacting with an internal hydrogen target in the Integrable Optics Test Accelerator (IOTA) being constructed at Fermilab in the Advanced Superconducting Test Accelerator (ASTA) facility. We calculate the beam loss rates due to single Coulomb scattering, neutralization, and nuclear interactions. An estimate of the expected transverse ionization cooling rate and multiple-Coulomb-scattering heating rate is given. The longitudinal heating of the beam due to the negative slope of the stopping power and to energy straggling is also estimated.

* e-mail: stancari@fnal.gov

† Fermi National Accelerator Laboratory (Fermilab) is operated by Fermi Research Alliance, LLC under Contract DE-AC02-07-CH11359 with the United States Department of Energy.

I. INTRODUCTION

Ionization cooling is a fast beam cooling process based on the interplay between the loss of momentum that a circulating beam experiences as it traverses an absorber and the reacceleration of the beam itself in radiofrequency cavities [1–3]. It is best suited for muons. For electrons and positrons, multiple scattering at low energies and bremsstrahlung at high energies dominate the interaction with the absorber. For hadrons, the method is usually limited by nuclear interactions with the target.

The IOTA ring at the Fermilab ASTA facility is being designed and constructed to study nonlinear integrable optics, optical stochastic cooling, and other beam physics concepts using 150-MeV electrons. The same magnetic rigidity ($B\rho = 0.5$ Tm) would match protons of a few MeV. Because a possible candidate for an IOTA proton source is the existing HINS RFQ, we concentrate on 2.5-MeV circulating protons ($B\rho = 0.23$ Tm) interacting with a gaseous hydrogen target.

For 2.5-MeV protons, nuclear interaction cross sections are small [2]. Longitudinally, due to energy straggling in the target and to the negative slope of the stopping power as a function of energy, the proton beam will be still be heated unless corrective measures are taken, such as a wedge-shaped absorber in a dispersive region or coupling with the transverse planes. For this reason, a machine with very large momentum acceptance is required, and fixed-field alternating-gradient (FFAG) accelerators have been suggested for this purpose [9].

In this note, we address the question of a possible ionization-cooling experiment in the IOTA ring.

II. DESIGN CONSIDERATIONS

A conceptual layout of the experiment is shown in Fig. 1. Protons with kinetic energy $U = 2.5$ MeV (momentum $p = 68.5$ MeV/c, velocity $\beta = 0.0729$) are injected in the IOTA ring (circumference $C = 38$ m, revolution frequency $f_{\rm rev} = 0.57$ MHz, revolution time $T_{\rm rev} = 1.74$ μs) with an initial emittance $\varepsilon_i^n = 0.14$ μm (normalized, rms) or $\varepsilon_i = 1.92$ μm (geometrical, rms), and initial momentum spread $\delta_i = 1 \cdot 10^{-3}$, corresponding to an energy spread $\Delta E = 4.99$ keV. Intensity is not critical for these purposes. To avoid space-charge issues, we will consider an initial beam current $I_p = 1$ mA, corresponding to $N_p = 1.09 \cdot 10^{10}$ circulating protons. In the experimental straight section of the IOTA ring, an internal H_2 gas-jet target is installed with a thickness of $\Delta z = 5$ mm and variable density. The optics of the ring can be arranged so that the amplitude function is $\beta^* = 1$ cm in the interaction region (corresponding to an rms beam size of $\sqrt{\beta^* \cdot \varepsilon_i} = 0.14$ mm) and it does not exceed $\beta_{\rm max} = 10$ m around the ring ($\sqrt{\beta_{\rm max} \cdot \varepsilon_i} = 4.38$ mm). The minimum aperture radius in IOTA is 25 mm. We assume a transverse ring admittance $A = 62.5$ μm and a

momentum acceptance $\delta_{\max} = 1 \cdot 10^{-2}$.

A. Ionization cooling rates, heating mechanisms and partitioning

The stopping power for protons in H_2 is shown in Figure 2 [6]. The middle plot shows the absolute value of the slope of the stopping power vs. kinetic energy. Because of the negative slope in our region of interest, in the absence of corrective measures ionization energy loss will tend to increase the energy spread of the beam and add to the effect of fluctuations (straggling).

Following Ref. [4], we calculate the sum of the ionization cooling partition numbers for the transverse (g_x, g_y) and longitudinal (g_L) planes:

$$\Sigma_g \equiv g_x + g_y + g_L = 2 + \frac{d\langle dE/dx\rangle/dE \cdot E \cdot \beta^2}{\langle dE/dx\rangle}. \tag{1}$$

This function is plotted in Figure 2. Because the function remains positive, cooling in all planes is possible in principle. However, for a uniform target thickness n_s and no coupling between planes, we have $g_x = g_y = 1$ and $g_L = -1.64$, which means transverse cooling and longitudinal heating. By adding horizontal dispersion $D_x \neq 0$ and a thickness gradient n_s' at the target, for instance, one may redistribute cooling between planes:

$$g_x = 1 - \frac{D_x n_s'}{n_s}; \;\; g_y = 1; \;\; g_L = \frac{d(\langle dE/dx\rangle)/dE \cdot E \cdot \beta^2}{\langle dE/dx\rangle} + \frac{D_x n_s'}{n_s}. \tag{2}$$

Analogous expressions hold in the case of vertical dispersion or of strongly coupled transverse oscillations.

For 2.5-MeV protons in H_2, the stopping power is $\langle dE/dx\rangle = 323.8$ MeV$\cdot$cm^2/g. Due to the limited momentum acceptance of the machine, the energy loss per turn $\Delta U = \langle dE/dx\rangle \cdot \Delta x$ should be small

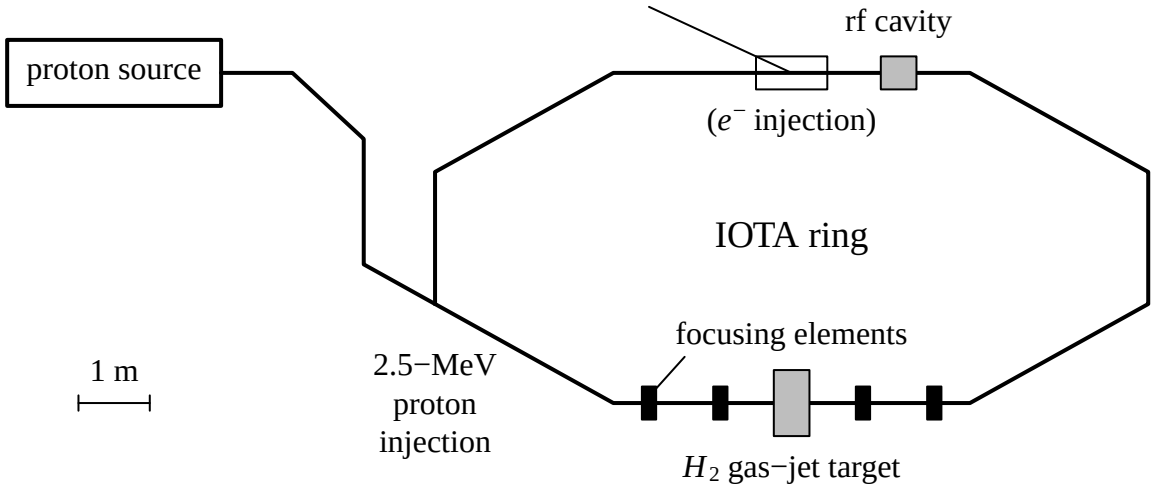

FIG. 1. Schematic layout of the apparatus.

compared to the kinetic energy U. We require $\Delta U/U < 1 \cdot 10^{-4}$ or $\Delta U = 0.25$ keV. This imposes a limit on the mass thickness of the target, $\Delta x = \Delta U/\langle dE/dx\rangle = 0.77\ \mu\mathrm{g/cm^2}$, corresponding to a number surface density $n_s = 4.61 \cdot 10^{17}$ atoms/cm^2, a density $\rho = 1.54 \cdot 10^{-6}$ g/cm^3, and a number density $n_v = 9.23 \cdot 10^{17}$ atoms/cm^3. (At room-temperature, the corresponding pressure is $P = 3.77 \cdot 10^1$ mbar).

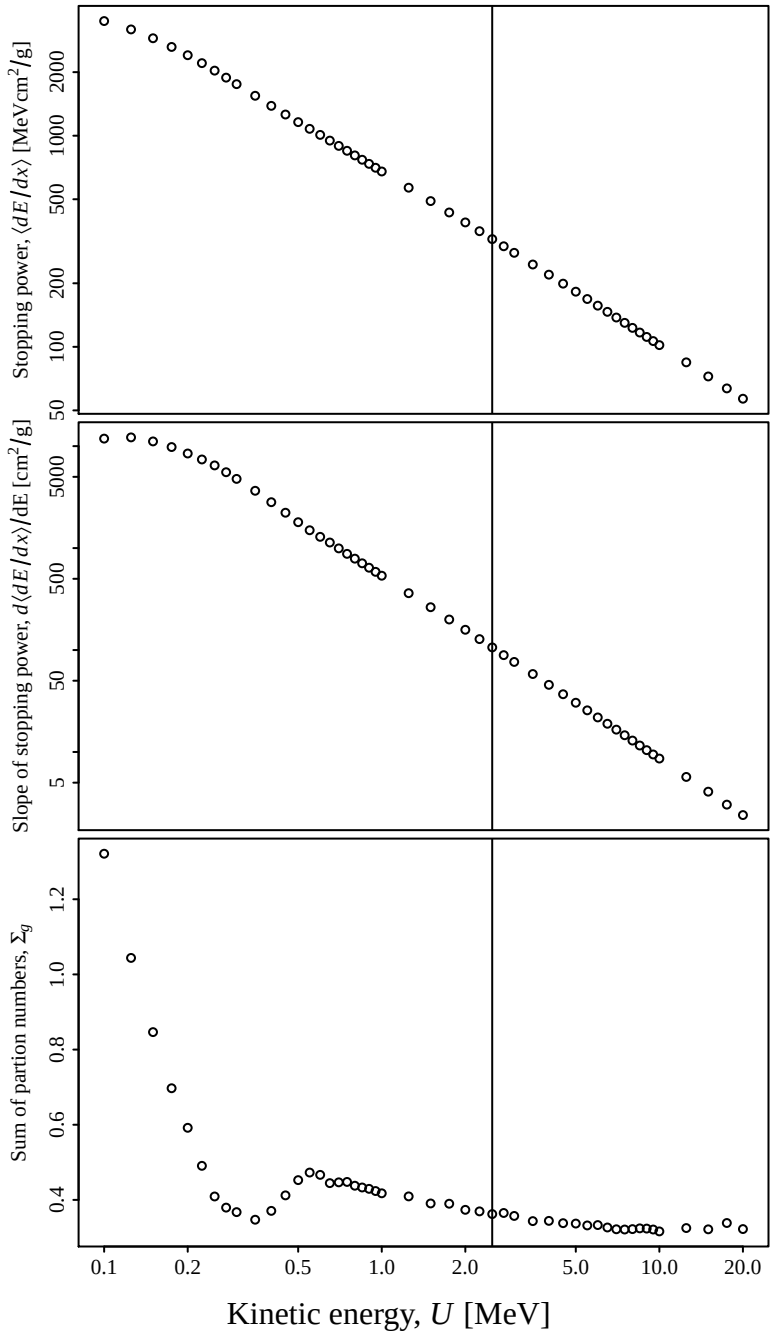

FIG. 2. Stopping power of protons in H_2 [6] (top plot); absolute value of the slope of the stopping power (middle); sum of the ionization cooling partition numbers (bottom).

Transversely, the rate equation for emittance evolution depends on the ionization heating/cooling rate A_t and on the heating term B_t due to multiple Coulomb scattering:

$$\dot{\varepsilon} = A_t \cdot \varepsilon + B_t. \tag{3}$$

The rate A_t and time $1/|A_t|$ depend on the total energy of the beam E, on the energy lost per turn ΔU, and on the revolution frequency $f_{\rm rev}$:

$$\begin{aligned} A_t &= -\frac{\Delta U \cdot f_{\rm rev}}{\beta^2 \cdot E} \simeq -\frac{\langle dE/dx \rangle \cdot \Delta x \cdot f_{\rm rev}}{2 \cdot U} = \\ &= -\frac{(0.25\ \text{keV}) \cdot (0.57\ \text{MHz})}{2 \cdot (2.5\ \text{MeV})} = -2.88 \cdot 10^1\ \text{s}^{-1} \\ \frac{1}{|A_t|} &= \frac{1}{3.48 \cdot 10^{-2}\ \text{s}} = \frac{1}{2 \cdot 10^4\ \text{turns}}. \end{aligned}$$

Multiple Coulomb scattering will tend to heat the beam. The radiation length of hydrogen is $X_0 = 63.04\ \text{g/cm}^2$, and $\Delta x/X_0 = 1.22 \cdot 10^{-8}$. We calculate the standard deviation of the projected angle using Highland's formula [7], as amended by Lynch and Dahl [8]:

$$\theta_{\rm rms} = \sqrt{\langle \theta_{x,y}^2 \rangle} = \frac{(13.6\ \text{MeV})}{\beta pc} \sqrt{\frac{\Delta x}{X_0}} \left[1 + 0.088 \log_{10} \left(\frac{\Delta x}{X_0 \beta^2} \right) \right] = 0.15\ \text{mrad}, \tag{4}$$

where is the radiation length of hydrogen. The corresponding heating rate B_t is proportional to the amplitude function in the interaction region:

$$B_t = \beta^* \cdot \theta_{\rm rms}^2 \cdot f_{\rm rev} = 1.33 \cdot 10^2\ \mu\text{m/s}. \tag{5}$$

We assume that, as long as $\theta_{\rm rms}^2 \sim \Delta x$, for the purposes of calculating the heating rate it is not relevant whether the assumptions of multiple Coulomb scattering are satisfied in a single traversal.

The combined action of ionization cooling and heating due to multiple scattering (Eq. 3) pushes the emittances towards an equilibrium value:

$$\varepsilon_\infty = -\frac{B_t}{A_t} = 4.61\ \mu\text{m}. \tag{6}$$

The solution of Eq. 3 describing the time evolution of transverse emittances is

$$\varepsilon(t) = \varepsilon_i \cdot \exp(A_t \cdot t) + \varepsilon_\infty \cdot [1 - \exp(A_t \cdot t)]. \tag{7}$$

If the initial emittance is larger that the equilibrium emittance, one can observe cooling directly. On the other hand, if the initial emittance is smaller than the equilibrium emittance, ionization cooling manifests itself as a fast damping of emittance growth.

Longitudinally, one can write a similar rate equation for the square of the energy spread $\sigma_{\rm E}^2$:

$$\dot{\sigma_{\rm E}^2} = A_l \cdot \sigma_{\rm E}^2 + B_l, \tag{8}$$

where both the ionization term A_l and straggling term B_l tend to widen the beam distribution:

$$\begin{aligned} A_l &= -2\frac{d\langle dE/dx\rangle}{dE}\cdot\Delta x\cdot f_{\rm rev} = 9.43\cdot 10^{1}\ \mathrm{s}^{-1} = \frac{1}{1.06\cdot 10^{-2}\ \mathrm{s}} \\ B_l &= 4\pi(r_e m_e c^2)^2\cdot n_s\cdot\gamma^2\left(1-\frac{\beta^2}{2}\right)\cdot f_{\rm rev} = 6.93\cdot 10^{-2}\ \mathrm{MeV}^2/\mathrm{s}, \end{aligned}$$

where $r_e = 2.82\cdot 10^{-15}$ m is the classical electron radius and $m_e c^2 = 0.51$ MeV is the electron's rest energy. In this case, the solution of Eq. 8 can be rewritten as

$$\sigma_{\rm E}^2(t) = \left(\sigma_{\rm Ei}^2 + \frac{B_l}{A_l}\right)\cdot\exp\left(A_l\cdot t\right) - \frac{B_l}{A_l}, \quad \text{with } \sqrt{\frac{B_l}{A_l}} = 27.11\ \mathrm{keV}. \tag{9}$$

The growth rate of the energy spread is vary large, causing quick particle loss and masking the effect of transverse cooling.

Through coupling, dispersion, and thickness gradients, one may redistribute the partition numbers so that $g_x' = 0.1$, $g_y' = 0.1$, and $g_L' = 0.16$. The cooling rates become

$$\begin{aligned} A_t' &= \frac{g_x'}{g_x}A_t = -2.88\ \mathrm{s}^{-1}; \quad \frac{1}{|A_t'|} = \frac{1}{3.48\cdot 10^{-1}\ \mathrm{s}} \\ A_l' &= \frac{g_L'}{g_L}A_l = -9.35\ \mathrm{s}^{-1}; \quad \frac{1}{|A_l'|} = \frac{1}{1.07\cdot 10^{-1}\ \mathrm{s}}, \end{aligned}$$

and the equilibrium emittance and energy spread are:

$$\begin{aligned} \varepsilon_\infty' &= -\frac{B_t}{A_t'} = 46.09\ \mu\mathrm{m} \\ \sigma_{\mathrm{E}\infty}' &= \sqrt{-\frac{B_l}{A_l'}} = 86.09\ \mathrm{keV} \end{aligned}$$

Under these conditions, the evolution of emittances and energy spreads is shown in Figure 3. Even in the case of cooling in all planes, a ring with large acceptance is required.

B. Particle losses

At these energies, the main sources of particle loss are large-angle single Coulomb scattering, charge exchange, and nuclear interactions.

The cross section for particle loss due to single Coulomb scattering is obtained by integrating the Rutherford cross section over the range of fatal kicks:

$$\sigma_{\rm SCS} = \left(\frac{2e^2}{4\pi\varepsilon_0 pc\beta}\right)^2\frac{\pi}{\theta_{\rm lim}^2} = 1.67\cdot 10^{-24}\ \mathrm{cm}^2, \tag{10}$$

where $\theta_{\rm lim} = \sqrt{A/\beta^*} = 79.06$ mrad is the maximum acceptance angle. (The atomic screening angle is negligible.) This cross section corresponds to the following loss rate:

$$\lambda_{\rm SCS} = \frac{1}{\tau_{\rm SCS}} = \sigma_{\rm SCS}\cdot n_s\cdot f_{\rm rev} = 4.43\cdot 10^{-1}\ \mathrm{s}^{-1} = \frac{1}{2.26\ \mathrm{s}}. \tag{11}$$

Charge exchange is one of the dominant processes. We extrapolate the ionization cross section $\sigma_{01} = 3.6 \cdot 10^{-17}$ cm^2 and the neutralization cross section $\sigma_{10} = 1.3 \cdot 10^{-23}$ cm^2 from Ref. [5]. Because the ionization process is much more likely than neutralization, most of neutralized protons will be reionized in the target. The mean free path of neutrals is $(\Delta z)_0 = 1/(n_v \sigma_{01}) = 0.3$ mm, so the effective neutralization thickness of the target is $(\Delta z)_0/\Delta z = 6\%$ and the neutralization rate is

$$\lambda_0 = \frac{1}{\tau_0} = \sigma_{10} \cdot n_s \cdot \frac{(\Delta z)_0}{\Delta z} \cdot f_{\text{rev}} = 2.08 \cdot 10^{-1}\ \text{s}^{-1} = \frac{1}{4.82\ \text{s}}. \tag{12}$$

It may be possible to exploit this flux of neutral hydrogen atoms to monitor the beam size with fluorescent screens, wire chambers, or microchannel plates placed after the first dipole magnet downstream of the target.

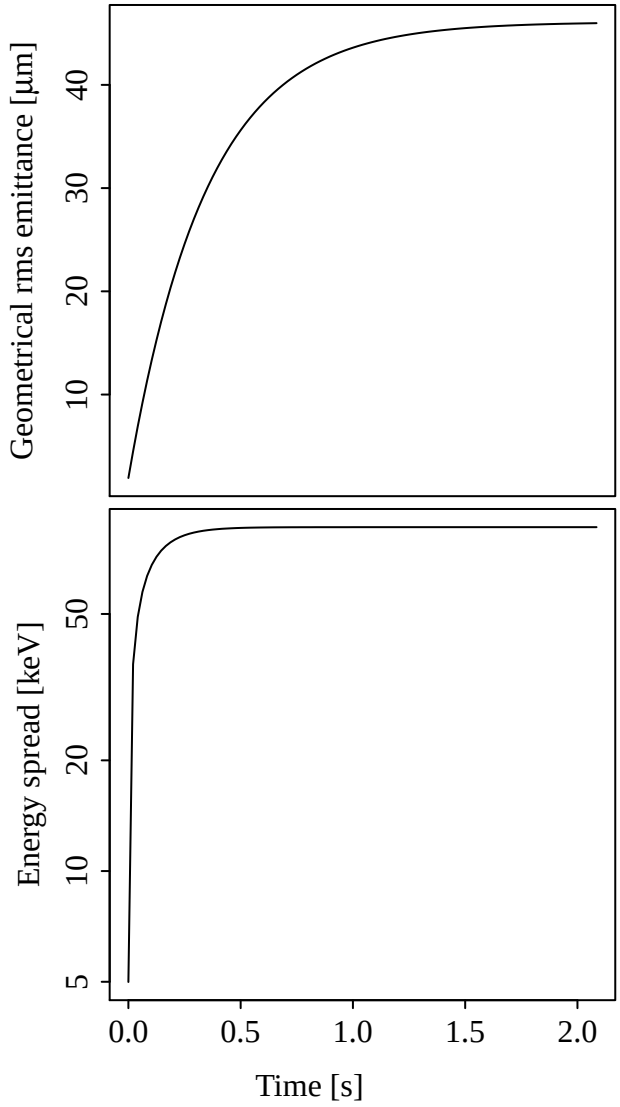

FIG. 3. Evolution of transverse emittances and energy spread.

For comparison, at these energies, the total nuclear proton-proton cross section is approximately $\sigma_N = 1 \cdot 10^{-24}$ cm^2, corresponding to a loss rate $\lambda_N = 2.65 \cdot 10^{-1}$ s^{-1} and a lifetime $\tau_N = 3.77$ s.

C. Observations

Because both cooling and heating rates are proportional to the target thickness, experiments should not be very sensitive to the detailed properties of the target. In a cell target, it may be possible to exploit the temperature gradients on the walls or the cell geometry to produce thickness gradients and attempt cooling in the longitudinal plane.

It is expected that emittance growth due to intrabeam scattering will be slow, but a more detailed study is needed to verify this assumption.

The low revolution frequency ($f_{\text{rev}} = 0.57$ MHz) and accelerating power ($q \cdot \Delta U \cdot I_p = 0.25$ W) disfavors the use of a conventional rf cavity for acceleration. A simpler modulation circuit may be used instead. Barrier buckets may also be investigated, and whether their use would substantially change the dynamics of ionization cooling.

III. CONCLUSIONS

This preliminary study suggests that a demonstration of ionization cooling in the IOTA ring at the Fermilab ASTA facility would be challenging. Without repartitioning, longitudinal heating would lead to fast particle loss, masking the effect of cooling. A redistribution of cooling between the transverse and longitudinal degrees of freedom may be possible, but the equilibrium emittances and momentum spreads still require a very large ring acceptance. In addition, beam lifetimes due to large-angle Coulomb scattering, nuclear interactions, and neutralization are of the order of a few seconds only.

[1] A. A. Kolomenskii, Atomic Energy **19**, 534 (1965).

[2] Yu. M. Ado and V. I. Balbekov, Atomic Energy **31**, 40–44 (1971).

[3] D. Neuffer, Part. Accel. **14**, 75 (1983).

[4] D. Neuffer, Nuclear Instrum. Methods Phys. Research A **532**, 26 (2004).

[5] C. F. Barnett and H. K. Reynolds, Phys. Rev. **109**, 355 (1958).

[6] M. J. Berger, J. S. Coursey, M. A. Zucker, and J. Chang, ESTAR, PSTAR, and ASTAR: Computer Programs for Calculating Stopping-Power and Range Tables for Electrons, Protons, and Helium Ions (version 1.2.3, 2005). [Online] Available: http://physics.nist.gov/Star [2013, February 1]. National Institute of Standards and Technol-

ogy, Gaithersburg, MD. Originally published as: M. J. Berger, NISTIR 4999, National Institute of Standards and Technology, Gaithersburg, MD (1993).

[7] V. L. Highland, Nucl. Instrum. Methods **129**, 497 (1975).

[8] G. R. Lynch and O. I. Dahl, Nucl. Instrum. Methods Phys. Research B **58**, 6–10 (1991).

[9] Y. Mori, Nuclear Instrum. Methods Phys. Research A **562**, 591–595 (2006).

[10] C. Rubbia, A. Ferrari, Y. Kadi, and V. Vlachoudis, Nuclear Instrum. Methods Phys. Research A **568**, 475–487 (2006).

[11] D. Neuffer, Nuclear Instrum. Methods Phys. Research A **585**, 109–116 (2008).